Available online at www.sciencedirect.com
SCIENCE DIRECT®
Journal of Crystal Growth 273 (2005) 347–356
JOURNAL OF CRYSTAL GROWTH
www.elsevier.com/locate/jcrysgro

An electrochemical study of photoetching of heteroepitaxial GaN: kinetics and morphology

L. Macht[a,*], J.J. Kelly[b], J.L. Weyher[a,c], A. Grzegorczyk[a], P.K. Larsen[a]

[a]*Experimental Solid State Physics III, RIM, University of Nijmegen, Toernooiveld 1, 6525 ED Nijmegen, The Netherlands*
[b]*Debye Institute, University of Utrecht Princetonplein 1, Utrecht, The Netherlands*
[c]*High Pressure Research Center, Polish Academy of Sciences, ul. Sokolowska 29/37, 01-142 Warsaw, Poland*

Received 26 May 2004; accepted 3 September 2004
Communicated by J.B.Mullin
Available online 13 October 2004

Abstract

Potentiostatic experiments in KOH solution were used to investigate the photoetching of the Ga-polar face of heteroepitaxial GaN layers grown on sapphire. Different etching regimes are identified; these depend on the applied potential, KOH concentration, light intensity and electron concentration. In particular, the importance of the relative rates of transport of photogenerated holes and OH^- ions to the surface for the etching kinetics and morphology is demonstrated. Consequently, the hydrodynamics of the etching system are important. These results form the basis for a comparison with a more widely used approach: photoenhanced open-circuit etching with a counter electrode.

PACS: 61.72.Ff; 61.72.Lk; 68.37.Hk

Keywords: A1. Etching; A1. Line defects; B1. Nitrides

1. Introduction

In the last decade, enormous progress has been made in both the growth and the characterization of gallium nitride. Products based on GaN are already available on the commercial market; these include light-emitting diodes, laser diodes, detectors and even a completely new standard for Home Entertainment—Blu-Ray. AlGaN/GaN-based high electron mobility transistors (HEMTs), having extremely high breakdown voltage and superior thermal and chemical stability, offer performance significantly better than that of GaAs-based devices. Despite all these advances, the scientific community still cannot say unequivocally that it has mastered the fabrication of GaN-based devices in all its aspects. The main reason remains the lack of a suitable growth

*Corresponding author. Tel.: +31 6485 06976; fax: +31 2436 52620.
E-mail address: lukasz@sci.kun.nl (L. Macht).

0022-0248/$ - see front matter © 2004 Elsevier B.V. All rights reserved.
doi:10.1016/j.jcrysgro.2004.09.029

substrate which is lattice matched to GaN. The production of single crystals, although possible, is still not efficient on a scale large enough to meet the market needs. The resultant crystals are not perfect; they have small dimensions and high intrinsic carrier concentration. Therefore, sapphire and silicon carbide (SiC) remain the substrates of choice for growth of GaN layers. Due to differences in lattice constants and thermal expansion coefficients the layers grown on these substrates contain a large number of threading dislocations. The average density for thin films grown on sapphire is around 10^9–$10^{10}\,cm^{-2}$ while it is an order of magnitude lower for samples grown on SiC. Despite this high dislocation density, manufactured devices function satisfactorily but their electrical and optical properties could be improved. The race for the perfect lattice is not over yet!

The only exact method for dislocation counting and general verification of the dislocation structure is still transmission electron microscopy (TEM). Unfortunately, a time-consuming and difficult specimen preparation and the need for expensive equipment make TEM unsuitable for routine use. Defect-selective etching constitutes an attractive alternative for fast assessment of the defect density. Two approaches have been successfully used for this purpose: photoenhanced wet etching [1,2] and etching in molten bases. The former method has a major drawback, namely its applicability depends upon the electrical characteristics of the etched material.

It was first shown by Minsky et al. [3] that n-type GaN, when illuminated, could be rapidly etched in KOH solution; no etching occurs in the dark. They suggested an etching process similar to that of GaAs, i.e. photogenerated holes cause oxidation and dissolution of GaN. Subsequently, in a series of articles, Youtsey et al. [1,4,5] showed that etching could result in both smooth and rough morphologies and they suggested a simplified reaction for the dissolution process. They also found a direct correlation between the surface morphology after etching and the concentration of the KOH solution. In addition, they showed that the resultant "whiskers" are, in fact, formed on dislocations. Weyher et al. [6] subsequently established a one-to-one correlation between whiskers and dislocation sites for Ga-polar layers and they also showed that whiskers are formed on narrow inversion domains in N-polar layers. In 2000, Rotter et al. [7] suggested a two-step process for etching of n-type GaN thin films grown by MOCVD on sapphire and a year later Nowak et al. [8] suggested the same mechanism for dissolution of GaN single crystals.

Much of the recent work on photoetching of n-type GaN in alkaline solution has been performed with a counter electrode (generally platinum) but without potentiostatic control of the semiconductor potential; a voltage source and reference electrode were, in general, not used [9]. An exception is the work of Borton et al. [10] and Huygens et al. [11].

Various factors are important in determining the etching kinetics and, thus, the surface morphology of the etched solid. These include the electrochemical potential of the semiconductor, the photon flux, the OH^- concentration in solution and the hydrodynamics of the system. If the potential of the semiconductor is not well defined then it is difficult to draw conclusions with regard to etching mechanisms and morphologies.

In the present work, we have studied the influence of the parameters listed above on the photoelectrochemical (PEC) etching of n-type GaN epitaxial films. These measurements allow us to define different etching regimes and their corresponding surface morphologies. In addition we try to relate this "potentiostatic" approach to the more commonly used "open-circuit" photoenhanced etching and we emphasize important differences between the two approaches. Finally, we indicate the range of dopant density for which photoetching of GaN is considered feasible.

2. Experimental procedures

A set of four GaN samples was grown by MOCVD on c-plane sapphire substrates. The substrates were first cleaned in $HCl:HNO_3$ solution outside the reactor and later annealed in N_2

atmosphere in the reactor while the temperature was ramped down from 1100 to 950 °C. A 90 nm low-temperature buffer layer was grown first at 525 °C, followed by the main GaN layer at 1175 °C. All the samples were Si-doped. Hall experiments, performed at room temperature, gave carrier densities of 1.5×10^{17}, 2.3×10^{18}, 4.6×10^{18} and $9.3 \times 10^{18}\,cm^{-3}$ (samples A, B, C and D, respectively). Ohmic contacts to the GaN were made by evaporating a Ti layer, 100 nm thick without any additional heat treatment. All the samples used in this study had a Ga-polar face.

Electrochemical measurements were performed in a three-electrode cell with a platinum counter electrode and a saturated calomel electrode (SCE) as reference. Potentials are given with respect to SCE; its potential is +0.24 V with respect to that of the standard hydrogen electrode (SHE). A potentiostat was used to measure current density—potential curves (j–U) in the dark and under illumination. In most of the experiments the potential was scanned at a constant rate (10 mV/s) and the (photo)current was measured as a function of potential. For details of such electrochemical measurements see Ref. [12]. The light source was a UV-enhanced xenon lamp with a power density of ~300 mW/cm^2 fitted with a water filter. It is important to note that this value was measured by an absorptive power meter in the whole emission range of the lamp while photoetching makes use only of the energy above the bandgap of GaN. Aqueous KOH solutions with a concentration varying from 0.001 to 0.05 M were used. Unless otherwise stated, the electrolyte solution was stirred during the experiment. For the measurement of the oxygen reduction current, the GaN working electrode was replaced by a Pt electrode.

For photoenhanced etching experiments the GaN working electrode was connected via an ammeter to the counter electrode, a platinum-coated plate. The etch rate and the morphology were studied as a function of carrier density and KOH concentration (0.001–0.5 M). The etching time was 20 min for all samples and, unless otherwise stated, the solution was stirred. All experiments described in this paper were performed at room temperature.

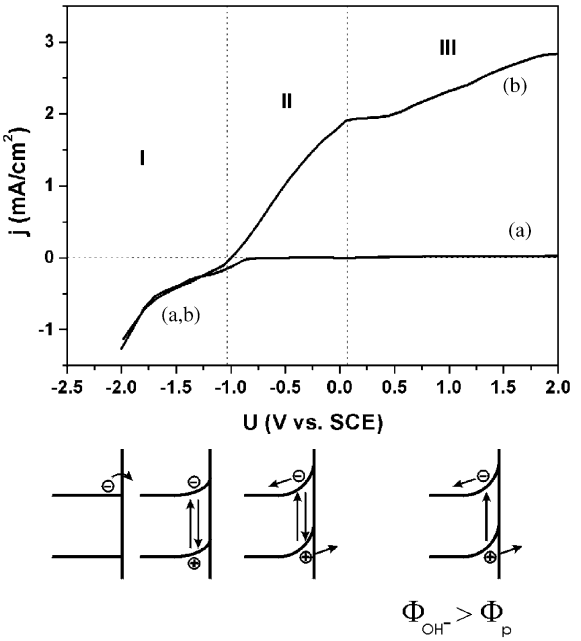

Fig. 1. Typical current density–potential plots for an n-type epitaxial GaN electrode: with a carrier concentration of $1.5 \times 10^{17}\,cm^{-3}$ in 0.004 M KOH solution: (a) in the dark and (b) under illumination. The corresponding energy band diagrams are also shown.

3. Results and discussion

3.1. Kinetics

Fig. 1 shows typical current density–potential plots for an n-type epitaxial GaN electrode with carrier concentration of $1.5 \times 10^{17}\,cm^{-3}$ in 0.004 M KOH solution at room temperature. In the dark (curve (a)) diode characteristics are observed. At negative potentials (range I) a cathodic current mainly due to hydrogen evolution results from the reduction of water by conduction band electrons [11,13].

$$2H_2O + 2e^- \rightarrow H_2 + 2OH^-. \quad (1)$$

The flat-band potential is located in this range ($U_{fb} = -1.4$ V), so that the electron concentration at the surface is high. At positive potentials the current is very low. Under illumination, electron–hole pairs are generated. In the potential range I the band bending is small and the electric field is

not sufficiently strong to separate the electrons and holes; they recombine both in the bulk and at the surface and, consequently, no photocurrent is observed. At more positive potential (stronger band bending in range II) a partial spatial separation of the charge carriers occurs. The holes driven to the surface can cause one of two electrochemical reactions: the oxidation of GaN,

$$GaN + 6OH^- + 3H^+ \rightarrow GaO_3^{3-} + 3H_2O + \tfrac{1}{2}N_2(g) \quad (2)$$

or the formation of oxygen,

$$4OH^- + 4H^+ \rightarrow O_2 + 2H_2O. \quad (3)$$

Previous work [11] has shown that dissolution of the semiconductor is the predominant reaction. The electrons are detected as a photocurrent in the external circuit (at the counter electrode they give rise to a reduction reaction e.g. hydrogen evolution). It is clear that in this potential range not all the photogenerated holes contribute to the photocurrent. Since the band bending is moderate, the surface electron concentration is still rather high and some recombination occurs. As the potential is made more positive, the recombination rate of electrons and holes decreases due to increase in the electric field and the photocurrent increases. In range III the photocurrent begins to level off. In Fig. 2 this photocurrent at 0.2 V is plotted as a function of the light intensity for a number of OH^- concentrations. At a given OH^- concentration (0.003 M for example) the photocurrent first increases linearly with light intensity and then becomes independent of the photon flux. This constant value at high intensity increases with increasing OH^- concentration. These results suggest that the photocurrent can be controlled in one of two ways. From Eq. (2) it is clear that OH^- ions are essential for the photoanodic reaction. If the flux of OH^- (Φ_{OH^-}) to the surface is larger than the flux of photogenerated holes to the surface (Φ_p), i.e. $\Phi_{OH^-} > \Phi_p$, then the photocurrent is determined by the light intensity. In this case the number of holes transferred across the semiconductor/solution interface per absorbed photon is high. This case corresponds to normal depletion, i.e. a change in applied potential (ΔU) results in a corresponding change of the space-charge layer potential ($\Delta U \approx \Delta U_{SC}$). If, on the other hand, the photon flux is high ($\Phi_{OH^-} < \Phi_p$), the OH^- ions at the surface will be depleted. In this case the rate of the surface reaction is determined by mass transport of OH^- ions and the limiting photocurrent depends on the pH of the solution and the hydrodynamics of the system. For example, if the solution is not stirred then a considerably lower photocurrent is observed. Since the rate of photogeneration of holes is higher than the rate of their reaction at the surface, considerable electron-hole recombination must occur, even in the limiting photocurrent range. The surface reaction is kinetically limited and the space-charge layer potential becomes independent of the applied potential (ΔU_{SC} = constant); because of accumulation of positive charge at the interface, the potential changes across the Helmholtz layer in solution ($\Delta U = \Delta U_H$) [14].

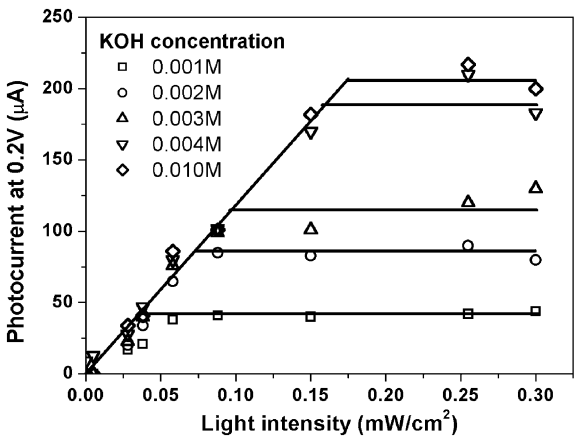

Fig. 2. The dependence of the photocurrent at 0.2 V on illumination intensity for different KOH concentrations. The electron density of the sample was $1.5 \times 10^{17}\,cm^{-3}$. Light intensity was measured for the full spectrum of the Xe lamp, however, only the range above bandgap energy of GaN can be used for photoetching.

When the KOH concentration is raised above 0.004 M only a slight increase in the photocurrent is observed at high intensity (see 0.01 M KOH in Fig. 2). An even higher OH^- concentration does not lead to a higher photocurrent. This result is very likely due to the formation of a sparingly

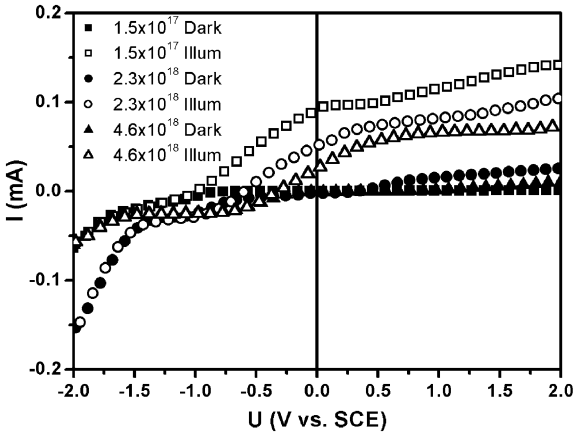

Fig. 3. Current–potential curves measured for three samples with different electron densities in the dark and under illumination in 0.004 M KOH solution.

soluble oxide [11].

$$2GaN + 6OH^- + 6H^+ \rightarrow Ga_2O_3 + 3H_2O + N_2. \quad (4)$$

Fig. 3 shows current–potential curves for n-type GaN electrodes with three dopant densities. The result for the lowest dopant density ($1.5 \times 10^{17}\,cm^{-3}$) has been discussed above. The results for the two higher dopant densities resemble those shown in Fig. 1. There are, however, two striking differences. An additional cathodic dark current is found with an onset at a potential more positive than that for hydrogen evolution. The process, which is more pronounced for the highest dopant density, is due to oxygen reduction by conduction band electrons.

$$O_2 + 2H_2O + 4e^- \rightarrow 4OH^-. \quad (5)$$

At a potential of $U \approx -0.75\,V$ a well-defined diffusion-limited current is clear in the case of the $4.6 \times 10^{18}\,cm^{-3}$ sample. The second difference with respect to the result for the lowest doped sample is the value of the onset potential for photocurrent: a shift to positive potentials is observed with increasing dopant density. This effect is caused by the difference in depletion layer width of the differently doped samples. During photoetching the excitation light is absorbed in a layer defined by the absorption coefficient and independent of the dopant density. Holes taking part in etching are generated either within the depletion layer itself or beyond the depletion layer but not further from the edge than the hole diffusion length [15]. The dopant density which controls the depletion layer width, thus controls the depth in the material from which photogenerated holes can take part in the etching and contribute to photocurrent. Therefore, at constant potential, a higher doped sample having a narrower depletion layer yields smaller photocurrent.

3.2. Open-circuit photoetching kinetics

In the experiments described in the previous section, the potential of the GaN electrode was fixed by the voltage source (potentiostat) and measured with respect to the reference electrode. In an open-circuit photoetching experiment (see Fig. 4(a)) the potential of the GaN is determined by the kinetics of the reactions occurring at both the semiconductor and the counter electrode. With short-circuited electrodes and no Ohmic losses in the system the Fermi level is constant (Fig. 4(b)). Holes produced by illumination of the semiconductor can either recombine with electrons or cause oxidation of the semiconductor. In the latter case the electrons pass to the counter electrode where a reduction reaction occurs. To maintain electroneutrality, the rate of the electrochemical reaction involving holes at the GaN/solution interface must be equal to the rate of reduction via electrons at the metal. The latter reaction is important in determining what happens at the GaN. In aqueous solution there are two possibilities for the reaction at Pt, the reduction of water

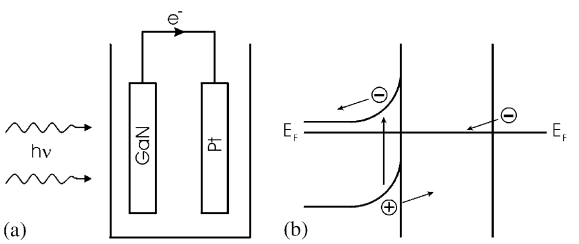

Fig. 4. Schematic representation of open-circuit photoetching (a) and of the energy bands and Fermi level of the GaN and Pt electrodes (b) under illumination.

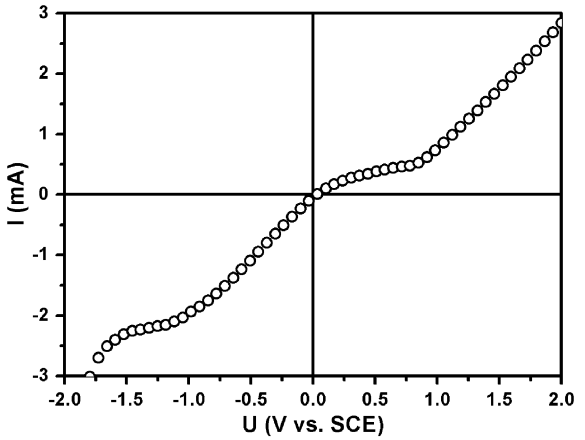

Fig. 5. Current–potential curve measured with a Pt working electrode in an aerated 0.004 M KOH solution. The solution was stirred.

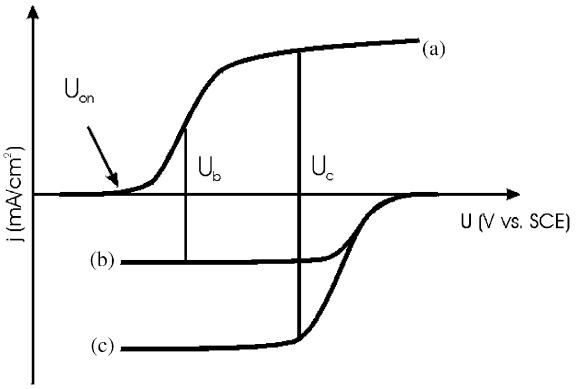

Fig. 6. Schematic current–potential curves illustrating the role of the counter electrode size in open-circuit photoetching. Curve (a) is the photocurrent–potential curve for GaN with onset potential U_{on}. Curves (b) and (c) refer to oxygen reduction at the counter electrode; the current in case (c) is larger than in (b) because of a larger surface area and/or more favourable mass transport condition. the corresponding open-circuit potentials are indicated by U_b and U_c.

(Eq. (1)) or of oxygen (Eq. (5)). For open-circuit photoetching to be possible, the onset of the reduction reaction must be at potential more positive than that of the photoanodic oxidation of GaN (−1.0 V in the case of low-doped sample, Fig. 1). To obtain information on which reduction reactions will be important we show in Fig. 5 the cathodic current–potential curve measured under potentiostatic conditions at a Pt electrode in stirred 0.004 M KOH solution. Oxygen reduction starts at 0 V, which is well positive of the photocurrent onset (see Fig. 1). The oxygen reduction current eventually becomes independent of potential since the reaction rate becomes mass-transport controlled. At more negative potential (−1.6 V) the cathodic current increases further; this is due to hydrogen evolution (Eq. (1)). This potential is more negative than the onset potential for photocurrent. Consequently hydrogen evolution is not important for photoetching under these conditions.

With regard to the counter electrode two factors are important: the electrocatalytic activity of the metal and the electrode area relative to that of the exposed GaN. To illustrate the latter aspect we consider two cases, depicted schematically in Fig. 6. Curve (a) is the photoanodic current–potential curve for an illuminated GaN electrode. Curves (b) and (c) represent oxygen reduction at a Pt counter

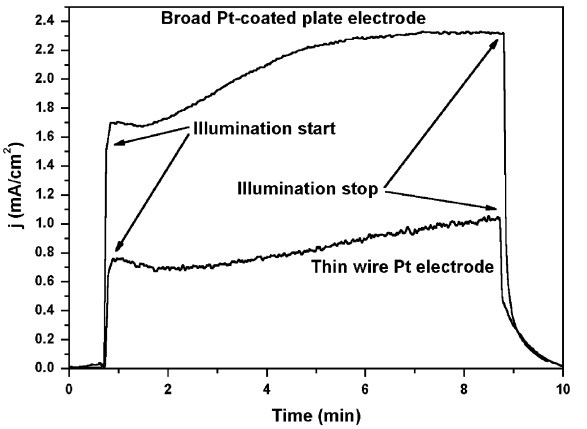

Fig. 7. The influence of counter electrode size on the measured photocurrent density for open-circuit photoetching.

electrode. In case (c) the mass-transport conditions are more favourable and/or the area of Pt is larger than in case (b). In the steady state the rates of oxidation and reduction must be equal. This defines the open-circuit potential of the system. From Fig. 6 it is clear that this potential can either be in the rising part of the photocurrent curve (U_b)

or in the limiting current range (U_c), depending on the area of the metal electrode, the kinetics of oxygen reduction at the metal and the hydrodynamics of the system. To illustrate the importance of surface area Fig. 7 shows results of photocurrent measurements as a function of time for an 8 min etching process using two different Pt electrodes, a thin wire with a surface area much smaller than that of the GaN electrode and a Pt-coated plate with an area roughly 50 times larger than that of the GaN sample. The results clearly illustrate the importance of counter electrode size on the photocurrent and therefore on the etch rate.

If there is a series resistance involved (for example, a poor Ohmic contact to GaN) the open-circuit situation becomes more complicated. There is an Ohmic potential drop across the resistance (see Fig. 8a) and the Fermi levels in semiconductor and counter electrode are no longer the same (Fig. 8b). This has consequences for the photoetching rate as is obvious from the schematic Fig. 9, which corresponds to the situation for curve (c) shown in Fig. 6. The etching rate is decreased markedly with respect to the resistance-free case. In fact, the potential of the semiconductor may be shifted substantially with a resulting change in etching mechanism (the Ohmic resistance displaces the potential from the limiting to the rising photocurrent range). Clearly, the latter effect may have consequences for the etching morphology.

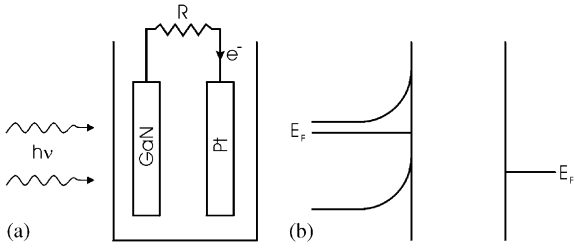

Fig. 8. Schematic representation of open-circuit photoetching (a) and the energy bands and Fermi level of the GaN and Pt electrodes (b) in the case of an additional Ohmic resistance (such as a low-quality contact to the GaN electrode).

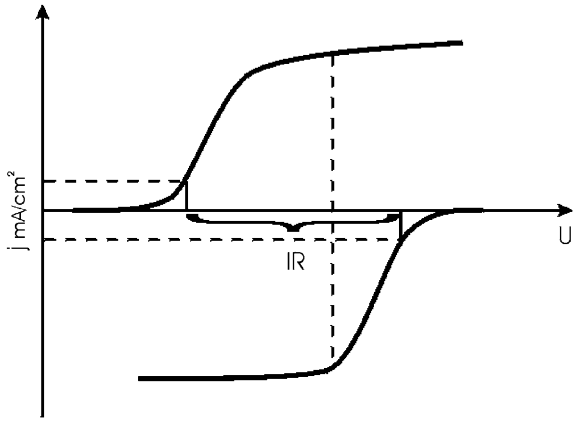

Fig. 9. Schematic current–potential curves illustrating the influence of an additional Ohmic resistance on open-circuit photoetching. The ohmic drop (IR) shifts the potential of the GaN to a more negative value, thereby decreasing the photoetching rate.

A comparison of Figs. 3 and 5 shows that the dopant density can be expected to influence the open-circuit etching rate. In fact, the measured etch rate is inversely proportional to the carrier concentration and amounts to 4 μm/h, 2.2 μm/h, 300 nm/h and <100 nm/h for the samples with electron concentrations 1.5×10^{17}, 2.3×10^{18}, 4.6×10^{18} and 9.3×10^{18}, respectively. This is due to the fact that at higher dopant density the onset of photocurrent is shifted considerably to the more positive potentials and the "overlap" between the anodic and cathodic curves becomes less favourable. This results in a lower open-circuit photoetching rate. The rate of 4 μm/h for the most favourable case (the lowest electron density) agrees reasonably well with that expected on the basis of the corresponding limiting photocurrent density (3.5 μm/h).

3.3. Morphology

The rate-determining step of the dissolution reaction generally decides the morphology of the etched surface [16]. In GaN photoetching one can clearly distinguish two main etching regimes: on the one hand, strong defect selectivity results in the formation of "needles" and, on the other hand, a uniform polishing of the surface is possible [17], Past experience with (photo)etching of III–V and other semiconductors helps us to relate surface morphology to the kinetics of the etching reaction. Recombination of photogenerated holes with

electrons reduces the dissolution rate at surface defects. This mechanism is responsible for the formation of needles at threading dislocations in GaN. Clearly these conditions correspond to potential range II of Fig. 1. Mass transport control of etching by species in solution usually results in polishing. Surface reactivity is not important. Since diffusion to protruding parts of surface is more effective than to recessed parts, a levelling action occurs. Polishing of GaN is expected in the limiting photocurrent range (III) when the flux of OH^- ions is rate-determining ($\Phi_{OH^-} < \Phi_p$). If oxide solubility is a problem, as at high photocurrent densities, then etching may become non-uniform due to local differences in the thickness and etching properties of the oxide. The result shown in Fig. 10 gives a nice illustration of how morphology can be determined. A fiberguide, placed close to the GaN surface, was used to photoetch a GaN sample under open-circuit conditions. A low KOH concentration (0.004 M) was used and the solution was not stirred. At the centre of the illuminated area the photon flux was clearly higher than the OH^- ion flux and smooth etching occurs. On the other hand, defect selective etching, clear from the appearance of needles, occurs at the edge of the illuminated area. This is due to an enhanced supply of OH^- ions from the surrounding non-etching area (outside the light spot) and, possibly, to a reduction of light intensity as a result of the Gaussian distribution in the beam. Improved hydrodynamics gives rise to a larger etch rate at the edge, as indicated by the deeper groove at the perimeter of the illuminated area (this is referred to as the negative crown effect).

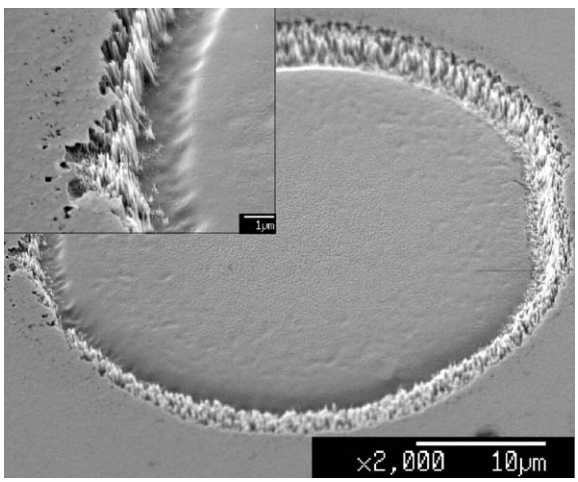

Fig. 10. A SEM micrograph demonstrating the results of open-circuit etching via fiberguide. Kinetically controlled etching near the edge reveals dislocations in the form of needles while the centre of the spot remains smooth as a result of mass-transport controlled etching.

Fig. 11 shows a series of SEM micrographs detailing defect-selective features for open-circuit etching with a range of KOH concentrations and GaN electron densities. Each micrograph shows an area of the sample that was partially covered by wax during etching. The wax has been subsequently removed to show the contrast between the morphology of etched and unetched areas. Two trends are clear. At constant KOH concentration (see, for example, 0.004 M) the etch rate drops with increasing electron density and defect selectivity is lost for the highest doped sample; the upper limit for open circuit photoetching is roughly $5 \times 10^{18}\,cm^{-3}$. For a given electron density a clear change in morphology is observed on going to higher KOH concentration. This is very likely related to the limitation of the photocurrent observed in Fig. 2 at high KOH concentration (>0.004 M). Oxide formation seems to prevent uniform etching of the surface and localized pits are formed, not related to defects.

The lower limit of carrier concentration is less easily defined. In the case of resistive samples uniform etching does not take place. In such a situation it is clear that the distance from the titanium contact will have an impact on the etch rate since the total resistance "seen" by the electrons is proportional to the distance travelled. The effect is similar to that introduced by a low-quality Ohmic contact (see Fig. 4). The practical lower limit of carrier concentration for uniform etching is roughly $10^{16}\,cm^3$. However, samples having an even lower carrier concentration can be PEC etched in narrow area near the Ti contact. This area is usually sufficient for a quick verification of dislocation density but it does not allow for a thorough study.

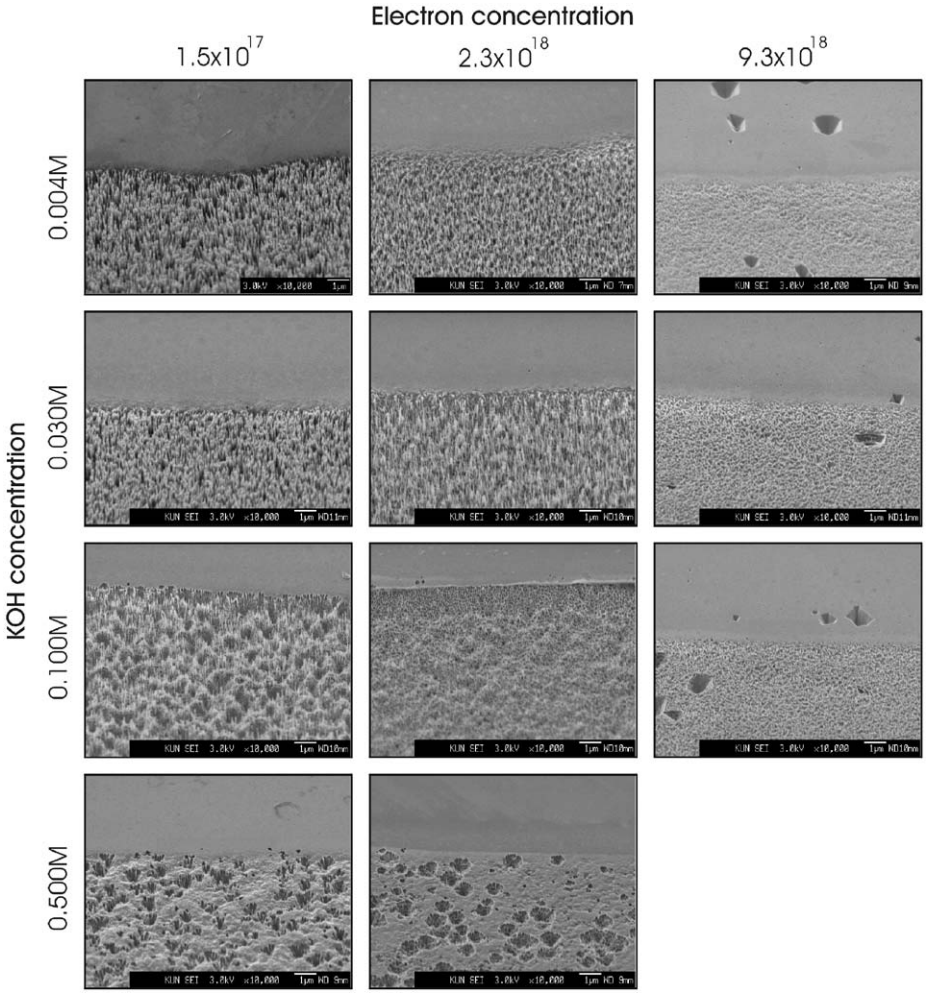

Fig. 11. PEC etching features as a function of electron concentration and KOH molar fraction.

4. Conclusions

Electrochemical experiments have shown that the anodic photocurrent of GaN can be controlled either by the photon flux or the OH^- ion diffusion rate. For sufficiently large KOH concentration, photocurrent and etch rate are linearly dependent on the intensity of absorbed light. However, if the KOH concentration is low then diffusion of OH^- ions rate becomes the limiting step and a further increase of light intensity does not yield a higher photocurrent or etch rate. In the first case we have a defect-selective regime since local depletion of holes at recombination centres such as dislocations leads to the creation of needles. The latter case leads to polishing-like behaviour and defect selectivity is lost. A transition between the two regimes can be realized by changing the KOH concentration and illumination intensity.

In the case of open-circuit experiments, matching of the anodic photocurrent at the GaN electrode with the cathodic current at the counter electrode sets the open-circuit potential. For samples with higher electron concentration this potential is in the rising part of the current-potential plot which limits the photocurrent and

etch rate. In addition, a low-quality ohmic contact or small-area counter electrode can introduce an extra series resistance in the circuit; this decreases the current and further lowers photoetch rate.

The practical range of electron concentration that can be expected to give valuable data falls between 10^{16} and $5 \times 10^{18}\,\mathrm{cm}^{-3}$. This also happens to be the natural electron concentration for unintentionally doped samples.

Acknowledgements

This work has been financially supported by Stichting voor Fundamenteel Onderzoek der Materie (FOM).

References

[1] C. Youtsey, L.T. Romano, R.J. Molnar, I. Adesida, Appl. Phys. Lett. 74 (1999) 3537.
[2] P. Visconti, K.M. Jones, M.A. Reshchikov, R. Cingolani, H. Morkoç, R.J. Molnar, Appl. Phys. Lett. 77 (2000) 3532.
[3] M.S. Minsky, M. White, E.L. Hu, Appl. Phys. Lett. 68 (1996) 1531.
[4] C. Youtsey, I. Adesida, G. Bulman, Appl. Phys. Lett. 71 (1997) 2151.
[5] C. Youtsey, L.T. Romano, I. Adesida, Appl. Phys. Lett. 73 (1998) 797.
[6] J.L. Weyher, F.D. Tichelaar, H.W. Zandbergen, L. Macht, P.R. Hageman, J. Appl. Phys. 90 (2001) 6105.
[7] T. Rotter, D. Mistele, J. Stemmer, F. Fedler, J. Aderhold, J. Graul, V. Schwegler, C. Kirchner, M. Kamp, M. Heuken, Appl. Phys. Lett. 76 (2000) 3923.
[8] G. Nowak, X.H. Xia, J.J. Kelly, J.L. Weyher, S. Porowski, J. Crystal Growth 222 (2001) 735.
[9] L.-H. Peng, C.-W. Huang, J.-K. Ho, C.-N. Huang, C.-Y. Chen, Appl. Phys. Lett. 72 (1998) 939.
[10] J.E. Borton, C. Cai, M.I. Nathan, P. Chow, J.M. Van Hove, A. Wowchak, H. Morkoç, Appl. Phys. Lett. 77 (2000) 1227.
[11] I.M. Huygens, K. Strubbe, W.P. Gomes, J. Electrochem. Soc. 147 (2000) 1797.
[12] P.H. Reiger, Electrochemistry, Prentice-Hall, Englewood Cliffs, NJ, 1987 (Chapter 4, Section 4.2).
[13] J.D. Beach, R.T. Collins, J.A. Turner, J. Electrochem. Soc. 150 (2003) A899.
[14] J.J. Kelly, P.H.L. Notten, J. Electrochem. Soc. 130 (1983) 2452.
[15] W.W. Gartner, Phys. Rev. 116 (1959) 84.
[16] P.H.L. Notten, J.E.A.M. van den Meerakker, J.J. Kelly, Etching of III–V Semiconductors: An Electrochemical Approach, Elsevier Advanced Technology, Oxford, 1991.
[17] C. Youtsey, I. Adesida, L.T. Romano, G. Bulman, Appl. Phys. Lett. 72 (1998) 560.